

SNOW COVER AND GLACIERS

DOI: 10.21782/EC2541-9994-2019-3(11-19)

ASSESSMENT OF GLACIER ALBEDO IN THE AK-SHYIRAK MASSIF
(INNER TIEN SHAN) FROM GROUND-BASED AND LANDSAT DATAD.A. Petrakov¹, O.V. Tutubalina¹, A.M. Shpuntova¹, N.V. Kovalenko¹, R.A. Usabaliev²,
E.A. Azisov², P.G. Mikhailukova¹¹ Lomonosov Moscow State University, Faculty of Geography, 1, Leninskie Gory, Moscow, 119991, Russia; dpetrakov@gmail.com² Central-Asian Institute for Applied Geosciences, 73/2, Timur Frunze str., Bishkek, 720027, Kyrgyz Republic

Albedo of glaciers in the Ak-Shyirak massif (Inner Tien Shan) has been estimated from ground-based and remote sensing data. The reduction of albedo typical to many ice-clad high mountain areas leads to accelerated downwasting of glaciers. The albedo values in the Ak-Shyirak area may bear an unconstrained effect of technogenic dust pollution. Ground-based albedo measurements were carried out across eleven glaciers during the summers of 2015 and 2016 using a Kipp&Zonen *Sp Lite 2* albedometer. On the basis of ground albedo measurements of two glaciers we developed a model to correct albedo values obtained from satellite imagery. 27 images from Landsat satellites were selected to assess glacier albedo in the Ak-Shyirak massif by weather conditions. Unlike other high mountain areas, the average glacier albedo in the Ak-Shyirak massif has not decreased since 1990s. Glacier albedo in the Ak-Shyirak massif is driven by environmental factors, mostly by weather conditions prior to satellite survey, especially snowfalls, and elevation driving the snow melting. Technogenic impact, such as mechanic disturbance of glaciers within the Kumtor gold mine, is detectable only locally. No mining-related dust pollution is traceable against the natural background across the Ak-Shyirak massif in *Landsat* data.

Albedo, mountain glaciers, Tien Shan, Ak-Shyirak massif, technogenic impact

INTRODUCTION

Albedo characterizes the reflectance of objects on the Earth's surface in a broad spectral range (visible light or visible+infrared wavelengths) at different observation angles. It is a key variable that controls the Earth's energy balance and has implications for climate and heat budget components of continental glaciers [Franch *et al.*, 2014]. In the summer time, glacier surface albedo is critical for snow and ice melting patterns and its estimation is an essential element in mass balance modeling.

The reflectance of ice and snow surfaces is strongly variable in space and time [Dumont *et al.*, 2011] and depends on the properties of ice and snow, surface roughness, distribution and number of patches, surface moisture, and radiation flux parameters [Warren, 1982; Aoki *et al.*, 2007; Jin *et al.*, 2008; Dozier *et al.*, 2009].

Albedo ranges from 0 to 1 and is normally as high as 0.9 for freshly fallen snow but only 0.2 [Warren, 1982; Oerlemans and Knap, 1998] or lower [Konovalov, 1985; Brock *et al.*, 2000] for dirty ice. It has been decreasing lately in some mountain systems worldwide because of dust pollution [Naegeli *et al.*, 2017].

The Tien Shan glaciers have high natural dust contents on the surface and, hence, low albedo [Konovalov, 1985], as a result of aeolian dust transport from the Central Asian deserts and semi-deserts. Dust emission is especially high in spring and fall in the deserts of Kara Kum, Kyzyl Kum, and Moyun Kum. As it was noted already in the 19th century, dust haze often observed in the Ak-Shyirak massif in the summer time consists of air-borne dust particles carried with accelerated western winds from desert areas [Kaulbars, 1875].

Dust may also come from bare surfaces in immediate vicinities of glaciers: valley sides or partly vegetated flat and shallow watersheds (locally called *syrt*). Steep slopes surrounded glaciers are responsible for most of dust input due to physical weathering [Glazovskaya, 1952].

Glaciers in the Ak-Shyirak massif have been exposed lately to impact from gold mining operated by the Kumtor Gold Company. Direct impact is mechanical displacement of ice in the Davydov glacier [Petrakov *et al.*, 2016; Torgoev, 2017], indirect impact is mining-related dust emission of 3–4 tons daily [Tör-

The English text is published as edited by the authors.

Copyright © 2019 D.A. Petrakov, O.V. Tutubalina, A.M. Shpuntova, N.V. Kovalenko, R.A. Usabaliev, E.A. Azisov, P.G. Mikhailukova, All rights reserved.

goev and Aleshin, 2001]. The dust emission was inferred [Kronenberg, 2013; Torgoev, 2017] to decrease the albedo of glaciers and to accelerate snow and ice melting, but the amount of dust produced by the Kumtor gold mining remained poorly constrained till recently. The contribution of mining to dust pollution has been apparently minor judging by precise analyses of dust concentrations in air [Kuzmichonok, 2012] and by the absence of correlation between glacier shrinkage rates and distance to the central pit [Petra-kov et al., 2016]. On the other hand, basing on data obtained in 2009 Torgoev [2017] concludes that the natural dust pollution of the glacier surface in the Kumtor mine area has been increasing as a result of cumulative dusting from the mine operation.

Currently, albedo is estimated by direct *in situ* field measurements or is retrieved from satellite observations, but the ground-based and remote sensing data lead to slightly different results [Knap et al., 1999; Lucht et al., 2000]. The remote sensing albedo assessment requires validation by ground-based data [Liang, 2001; Liang et al., 2003]. Ground albedo surveys over large territories often reveal variations caused by changes in the surface properties. Another pitfall consists in limited choice of measurement points, both in space and in time. The remote sensing data are free from biases caused by local seasonal variations and space-time limitations common to the ground-based data. Furthermore, the quality of satellite-derived albedo estimates can be improved by validation.

Goal of the study is an assessment of glacier surface albedo in the Ak-Shyirak massif using ground-based and *Landsat* data. Correspondingly, the objectives included acquisition, selection, and processing of multispectral *Landsat* images of the Ak-Shyirak areas from the early 1990s through 2016; ground-based albedo measurements in several glaciers in 2015–2016; estimation of remote sensing albedo using existing algorithms and validation using ground-based data; constraining the contribution from the Kumtor gold mining to the dust pollution of the Ak-Shyirak glaciers by analysis of spatiotemporal albedo variations.

METHODS

Ground-based albedo measurements

The ground-based measurements of albedo were performed using a Kipp&Zonen *SP Lite 2* albedometer consisting of two *SP Lite 2* pyranometers designed specially for field measurements of radiation [Solar Radiation Measurements, 2018; The Eppley Laboratory, 2018]. It is lightweight (0.32 kg), stable to external impacts (silicon instead of glass) and can run continuously with a specified frequency or in the on-off mode. The system includes two *Meteor* loggers that can record and/or read data and a 0.3 m holder. *SP Lite 2* is remarkable by very short response time (<500 ns) and high precision. The short response time, small weight, and a level gauge reduce leveling errors. The uncertainty includes <1 % nonlinearity



Fig. 1. Location map of ground-based albedo measurements (areas and points) in glaciers of Kyrgyzstan in 2015–2016.

1, 2 – glaciers covered with *in situ* albedo measurements of 2016 and 2015, respectively; 3 – national frontier of Kyrgyzstan; 4 – location of inset area. Inset enlarges fragments of the Ak-Shyirak and Jetimbel glacier areas covered with *in situ* albedo measurements.

Table 1. Data of ground-based albedo measurements in 2015–2016

Glacier and its number	Number of measurements	Cloud cover	Date	Central pit to glacier center distance, km	Mean arithmetic albedo of ice	Rms error
27	56	Partly cloudy	12.08.2015	15.6	0.18	0.03
354	91	»	13.08.2015	7.2	0.17	0.05
354	209	»	20, 22.07.2016	7.2	0.24	0.07
434	68	Sunny	14.08.2015	26	0.16	0.04
599	50	Partly cloudy	14.08.2016	145	0.23	0.06
Abramov	78	Sunny	02.08.2016	600	0.13	0.04
Adygene	121	»	10–11.07.2016	325	nd	nd
Golubin	98	»	28.08.2016	315	0.18	0.09
West Suyok (419)	70	Partly cloudy	14.08.2015	37.2	0.16	0.03
West Suyok (419)	81	»	16–17.08.2016	37.2	0.20	0.04
Lysyi	130	»	06.08.2015	3.4	0.18	0.05
Petrov	49	»	07.08.2015	8.2	0.16	0.04
Sary-Tor	194	»	05.08.2015	3.2	0.17	0.06

Note: nd = no data (snow on glacier surface).

error at radiation from 0 to 1 kW/m²; 0.15 %/°C temperature fluctuations in the –30 to +70 °C range; <2 % per year instrument instability [*SP Lite 2, 2015*]. Our data acquired within a short campaign of 45 days within a temperature range of 0 to +10 °C were free from instrument error and had minor temperature dependence, while the measurement error was 1.5 % or twice lower than the maximum of 3 % as per the manufacturer [*SP Lite 2, 2015*]. More precise measurements are possible only with stationary monitoring at weather stations. Both the pyranometers and loggers were calibrated by *Kipp&Zonen*.

Albedo of glaciers changes under increasing dust pollution. To pick this effect, we carried out route and areal surveys on seven glaciers in the Ak-Shyirak massif and in the Dzhetimbel Range in the summer of 2015 (Fig. 1), assuming distance-dependent contribution of the Kumtor central pit, which emits the greatest amount of technogenic dust, to the total dust pollution [*Torgoev, 2017*]. The selected glaciers (Sary-Tor, Lysyi, Petrov, No. 354 (South Bordu), No. 27 in the Tez River catchment, West Suyok, and No. 434) are located at a distance from 3 to 37 km away from the pit. The survey in 2016 covered several glaciers in the Kyrgyz (Adygene and Golubin), Alay (Abramov), Kyungei Ala-Too (No. 599), and Dzhetimbel (West Suyok) ranges and in the Ak-Shyirak massif (No. 354) in Kyrgyzstan (Fig. 1). The surveys aimed at correlating ground and remote sensing albedo. During route surveys, we tried to cover lower parts of glaciers completely to provide representative statistics for the ice surface. The dates of surveys, number of points, and cloud conditions are summarized in Table 1. The ice albedo show lognormal distribution in all cases, with ≤0.01 difference between the arithmetic mean and median values.

All points were navigated using a *Garmin 70 csx* portable GPS receiver and characterized in terms of surface features: ice (dirty, relatively dirty or clean), superimposed ice, firn, snow, and fresh snow.

The albedo survey of 2015 included areal coverage of the Sary-Tor and Lysyi glaciers and route measurements in other glaciers: altogether 658 measurements at 530 points. In 2016 albedo was measured at 603 points on a network of routes (637 samples). Albedo was measured several times at one point where the albedo values differed markedly within 2–3 m apart, and the arithmetic mean value was used for further calculations.

Albedo retrieval from Landsat data

Summer-time *TM/Landsat-5, ETM+/Landsat-7*, and *OLI/Landsat-8* images acquired from 1990 to 2016 were used to estimate albedo and analyze its spatial variations. Finally, 27 scenes of the Ak-Shyirak area were selected (Table 2) from more than 200 images. All scenes satisfied the conditions of warm season, clear sky (rare to absent clouds), and minimum fresh snow on the glaciers; all images with new snow were rejected. Additionally, we used several scenes of the Abramov, Adygene, and Golubin glaciers obtained in the summer of 2016 concurrently with *in situ* measurements.

Atmospheric correction according to the USGS guide [*USGS, 2018*] was applied for all images, then they were converted to surface reflectance mode.

Retrieval of albedo from satellite imagery (multispectral *Landsat* data) begins with the choice of algorithm and its calibration using ground-based data. To choose the optimal algorithm, we analyzed several empirical equations to estimate total ice and snow albedo from multispectral *Landsat* data (Table 3). The

Table 2. *Landsat* scenes used for albedo assessment at the Ak-Shyrak glaciers

Number	Scene ID	Date	Average albedo	δ^*
1	LT51480311991263	20.09.1991	0.60	9.4
2	LT51480311993268	25.09.1993	0.55	4.7
3	LT51480311997199	18.07.1997	0.32	0.1
4	LT51480311998234	22.08.1998	0.53	14.4
5	LE71480311999197	16.07.1999	0.37	105.7
6	LE71480311999261	18.09.1999	0.37	22.8
7	LE71480312001250	07.09.2001	0.58	7.2
8	LE71480312002205	24.07.2002	0.48	1.8
9	LE71480312002237	25.08.2002	0.31	0.0
10	LT51480312006224	12.08.2006	0.32	0.03
11	LT51480312006256	13.09.2006	0.52	2.1
12	LT51480312007195	14.07.2007	0.57	33.0
13	LT51480312007211	30.07.2007	0.41	1.9
14	LT51480312007259	16.09.2007	0.36	0.02
15	LT51480312008166	14.06.2008	0.47	1.4
16	LT51480312009136	16.05.2009	0.61	82.5
17	LT51480312010251	08.09.2010	0.46	4.2
18	LT51480312011254	11.09.2011	0.58	8.9
19	LC81480312013211	30.07.2013	0.33	0.1
20	LC81480312013243	31.08.2013	0.57	2.3
21	LC81480312013275	02.10.2013	0.50	0.07
22	LC81480312014134	14.05.2014	0.49	0.07
23	LC81480312014182	01.07.2014	0.39	0.2
24	LC81480312015169	18.06.2015	0.61	0.01
25	LC81480312015185	04.07.2015	0.48	0.8
26	LC81480312015233	21.08.2015	0.30	1.2
27	LC81480312016172	20.06.2016	0.57	0.09

* Percentage of bad pixels, %.

data of Table 3 along with band designations for the *Landsat* imagery [What are the band..., 2018] show that equation (1) from [Liang, 2001] uses too high reflectance in the visible waveband, as well as equation (3) of Brest and Goward [1987] which includes the greatest weight of green band in visible light. In this respect, better accuracy can be achieved with near- and medium-infrared reflectance as in equations

(2)–(4) which are used in our further consideration (Table 3).

Thus, albedo was estimated using equations (2)–(4) and *ERDAS Imagine 2016* software.

To choose the optimal equation and calibrate the respective algorithm, the albedo values retrieved from *OLI/Landsat-8* data were validated using ground *in situ* measurements.

Data matching and correction

Verification of satellite-derived albedo against ground-based data requires special caution about the time difference between *in situ* and satellite sampling because albedo is highly variable even in relatively stable weather [Knap et al., 1999]. The ideal time between the satellite overpass and ground measurements is less than 3 hours from both measurements and astronomical noon [Knap et al., 1999; Pimentel et al., 2016]. During stable weather, in the absence of snowfall and melt/freeze processes at the glacier surface, ground measurements can be performed in a few days before or after the satellite overpass but the time difference with astronomical noon should be less than 3 hours [Knap et al., 1999].

Since peak of precipitation in the Inner Tien Shan is observed during summer, only a limited amount of data could be used to compare the ground and satellite albedo. In 2016, albedo was measured *in situ* at the Adygene, Golubin (Kyrgyz Range) and Abramov (Alay Range) glaciers at clear sky on the days of *Landsat 8* overpass. The multispectral *Landsat 8 OLI* scenes have a 30 m pixel size and a geolocation error of 12 m [Storey et al., 2014]. The calculated (Table 3) and measured albedo was correlated statistically; the regression equations were derived using best fit values (<0.1 misfit between ground-based and satellite-derived albedo). Worse fit was observed at the glacier margins, at sharp (within a pixel) transitions between high albedo in ice and low values in debris cover. Thus, the margin pixels were interpreted as mixed ones. The satellite albedo was further calibrated using regression equations for the Abramov glacier which had the best quality of ground data: only 2 points out of 78 or <3 % were rejected (com-

Table 3. Regression equations to assess albedo from *Landsat* data

Sample	Equation (b_n is n -th band)*		Reference
	<i>Landsat 5 TM, Landsat 7 ETM+</i>	Adapted for <i>Landsat 8 OLI</i> data	
(1)	$0.443b_1 + 0.317b_2 + 0.240b_3$	$0.443b_2 + 0.317b_3 + 0.240b_4$	[Liang, 2001]
(2)	$0.526x1.12b_4 + 0.232b_4 + 0.130x0.63b_4 + 0.112xb_7$	$0.526x1.12b_5 + 0.232b_5 + 0.130x0.63b_5 + 0.112xb_7$	[Duguay and LeDrew, 1992]
(3)	$0.493b_2 + 0.203b_4 + 0.150b_5 + 0.154b_7$	$0.493b_3 + 0.203b_5 + 0.150b_6 + 0.154b_7$	[Brest and Goward, 1987]
(4)	$0.782b_4 + 0.148b_4^2$	$0.782b_5 + 0.148b_5^2$	[Knap et al., 1999]

* Bands for *Landsat 5 TM* and *Landsat 7 ETM+* systems: b_1 = blue, b_2 = green, b_3 = red, b_4 = near infrared, b_5, b_7 = average infrared; for *Landsat 8 OLI*: b_2 = blue, b_3 = green, b_4 = red, b_5 = near infrared, b_6, b_7 = average infrared.

Table 4. **Albedo assessment from ground-based and *Landsat* data for reference glaciers of Abramov and Adygene**

Glacier	Survey date	Surface	Number of measurements	Regression equation for <i>Landsat</i> data	Number of measurements*	Regression equation for ground-based data**	Correlation coefficient (<i>R</i>)	Rms error (σ)
Abramov	03.08.2016	Ice	78	(2) [<i>Duguay and LeDrew, 1992</i>]	76	$0.913a + 0.03$	0.66	0.02
Adygene	11.07.2016	Snow	122	(2) [<i>Duguay and LeDrew, 1992</i>] (4) [<i>Knap et al., 1999</i>]	87 89	$0.938a + 0.05$ $0.812a + 0.08$	0.75 0.72	0.05 0.05

*without data of >0.1 misfit.

** *a* is albedo from *Landsat* data.

pare with 32–34 out of 121 or 28 % of points rejected in the Adygene glacier). Generally, the misfit over the total area of glaciers was less than 0.1, i.e., the ground vs. satellite albedo correlation approach is well applicable to homogeneous surfaces.

On the other hand, the albedo calculated by equation (1) from [*Liang, 2001*] (Table 3) showed rather poor correlation with ground data from the Golubin glacier which had an inhomogeneous surface of fresh snow patches on ice on the day of measurements (28 August 2016).

During our surveys, the weather conditions were stable and the satellite data were acquired at clear sky for the Abramov and Adygene glaciers only. The glacier surface was quite homogeneous in the absence of night freezing or rainfall due to warm anticyclonic weather. Thus, the final statistical analysis was applied to data from the Abramov (ice) and Adygene (snow) glacier surfaces (Table 4).

The calculations were performed using equation (2) of [*Duguay and LeDrew, 1992*] for both glaciers and equation (4) [*Knap et al., 1999*] for the snow surface of the Adygene glacier in order to check whether the latter equation can lead to better estimates. Equation (2) gave a slightly better fit than equation (4) and was finally chosen for correlation of satellite-derived and ground albedo assessment. Note that equation (2) [*Duguay and LeDrew, 1992*] applies only to the near infrared band data (which still bear effects of too high reflectance in *TM/Landsat-5* and *ETM+/Landsat-7* scenes).

Thus, satellite-derived albedo was calibrated against ground-based data using the respective empirical regression equation for the Abramov glacier providing the best fit:

$$a_{\text{land}} = 0.913a_{\text{sat}} + 0.03,$$

where a_{sat} was calculated by the equation from [*Duguay and LeDrew, 1992*].

Thus, calculations using equation (2) [*Duguay and LeDrew, 1992*] and corrections according to the empirical relationship based on ground measurements provide the most accurate model for retrieval of ice albedo of the Ak-Shyirak area from *Landsat* data.

All *Landsat* scenes of the Ak-Shyirak glaciers acquired for 1990–2016 were processed using the chosen equation 2 (Table 3) and the empirical regression equation for the Abramov glacier (Table 4).

The obtained albedo was additionally normalized to elevations in order to account for uneven illumination of the surface topography, but we eventually refused this step because the normalized data showed numerous artifacts associated with *ASTER Global DEM 2* errors common to rugged terrains.

The albedo distribution in the Ak-Shyirak glaciers was mapped based on calculated and visualized values within the glacier limits of 2013 [*Petrakov et al., 2016*] for scenes after 2008 and within the limits of 2003 for older scenes. The cloudy fragments were excluded using a cloud mask supplied together with images corrected for atmospheric effects; in the case of poor mask quality, the clouds were digitized manually.

RESULTS

Albedo distribution according to ground-based measurements

The distribution of albedo measured by areal ground-based surveys in 2015 was studied with the examples of the Sary-Tor and Lysyi glaciers and complemented with route measurements across other glaciers presented as mean arithmetic ice and snow albedo for each glacier. The variations of both ice and snow albedo values across glaciers are quite moderate (Table 1).

The Sary-Tor glacier albedo values (Fig. 2) do not show any distinct patterns, low albedo could be observed at lower part of glacier snout as well as in upper part of the glacier near the equilibrium line. High albedo is registered at patches of snow and superimposed ice. Mapping of albedo with contour lines at every 0.05 leads to a similar result.

Albedo on the Lysyi glacier (Fig. 3) was generally higher than in Sary-Tor, with low values localized at elevations of 4100–4400 m in the right-hand side of the glacier. The low albedo may be related to proximity of an eroded slope covered with abundant fine-grained and dust material. Like the Sary-Tor case, a

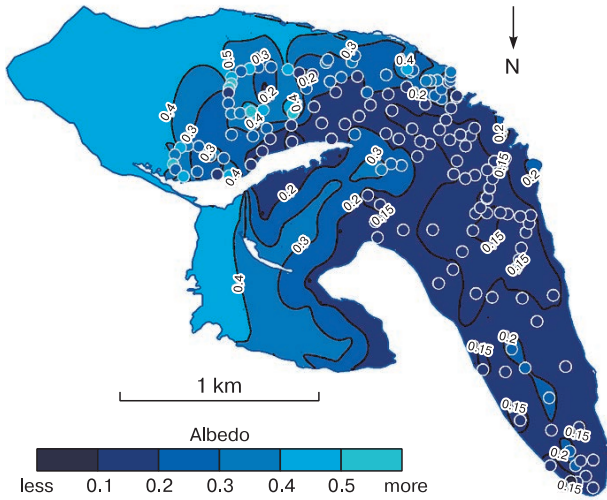


Fig. 2. Distribution of albedo at the Sary-Tor glacier (Ak-Shyirak massif) from ground-based measurements of 05.08.2015.

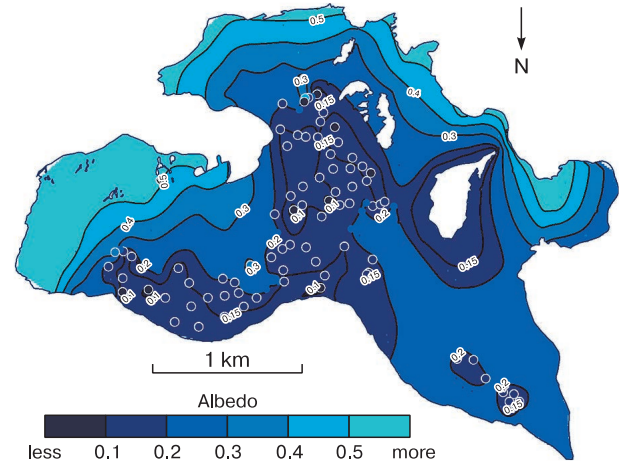


Fig. 3. Distribution of albedo at the Lysyi glacier (Ak-Shyirak massif) from ground-based measurements of 06.08.2015.

narrow zone of high albedo occurs in the middle of the Lysyi glacier, possibly because it is the most distant from the slopes and has clearer ice on the surface.

Elsewhere in the Ak-Shyirak glaciers, mean ice albedo was generally low in 2015 and varied from 0.16 in West Suyok to 0.18 in the Lysyi and No. 27 glaciers (Table 1). All variations of mean ice albedo for measured glaciers are within instrumental error and do not show any decreasing trend toward the central pit. Therefore, mining-induced dust emission remains undetectable against the natural background.

The average albedo for the ~2 km² of Abramov glacier surface (0.13) according to data of 2016 is much lower than those obtained for other glaciers in 2015 and 2016 (Fig. 4; Table 1). There are two possible reasons: (i) absence of snowfalls before the measurements and (ii) proximity of the Ferghana valley

as an additional source of dust. The value for the Golubin glacier is slightly higher but still low (0.18).

Average albedo for glaciers 599 (statistically significant data available for ice only) and 354 are 0.23 and 0.24. Note that the albedo of glacier 354 changed markedly from 0.21 to 0.27 in two days when water partially froze on the glacier surface in the night time.

Albedo distribution according to satellite data

The selected *Landsat* scenes were used to map the distribution of albedo over the whole area of the Ak-Shyirak glaciers (Fig. 5). This distribution is controlled by the absence or presence of snow which, in its turn, depends on elevation. Albedo is the lowest in hypsometrically low parts of the large glaciers Petrov, Jaman-Su, North Karasai and others.

To check the hypothesis of mining-induced dust effect, the albedo of the Ak-Shyirak glaciers were plotted as a function of distance from the central pit for each *Landsat* scene. Each point in the plot, one of more than 400,000 pixels, was presented as a pair of albedo-distance coordinates. Obviously, a prominent mining-induced effect would appear as high correlation between the albedo and distance values: the shorter the distance the lower the albedo. Yet, the correlation (*R*) is about zero in most of the cases. It is positive in only two out of 27 cases and negative in 13 cases, i.e., the albedo is rarely proportional to the distance from the central pit, and the inverse correlation (albedo increasing toward the quarry) is likewise quite poor. The relatively closer negative than positive correlation (6.5 times more cases) proves that the albedo of the Ak-Shyirak glaciers is almost unaffected by the Kumtor mining.

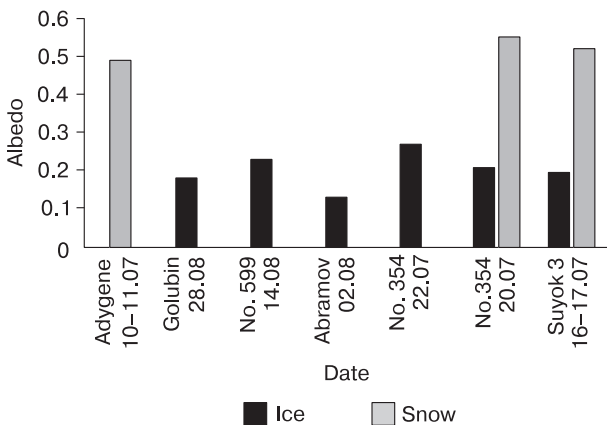


Fig. 4. Average snow and ice albedo values for surveyed glaciers of Kyrgyzstan in 2016.

The average albedo of the Ak-Shyirak glaciers retrieved from each *Landsat* scene vary notably (Table 2) depending on the presence or absence of new or spring snow. They are lower in July–August and early

September and higher in May–June and in the second half of September. Albedo in the Ak-Shyirak area do not show any decreasing trend contrary to those reported for the Alps [Brock *et al.*, 2000; Oer-

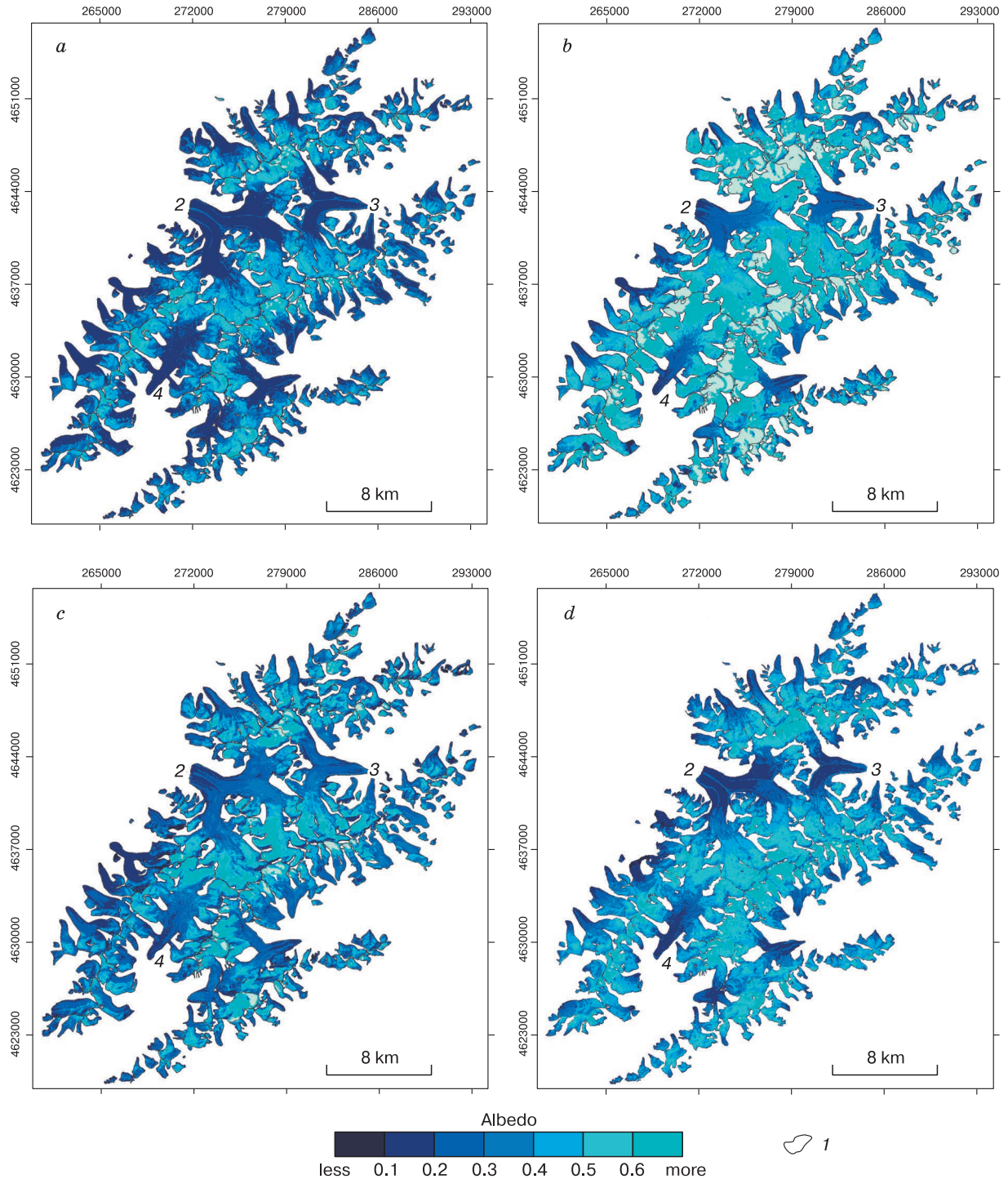


Fig. 5. Distribution of albedo across the Ak-Shyirak glaciers retrieved from *Landsat* data of different years. *a*: Landsat 5 TM, 04.09.1997; *b*: Landsat 7 ETM+, 24.07.2002; *c*: Landsat 5 TM, 16.09.2007; *d*: Landsat 8 OLI, 01.07.2014. 1 – glacier outlines; 2 – Petrov glacier, 3 – Jaman-Su glacier, 4 – North Karasai glacier. Coordinates are given in UTM Projection (Universal Transverse Mercator).

lemans et al., 2009], Greenland [As et al., 2012], and Tibet [Fujita and Ageta, 2000; Fujita, 2008a,b; Li et al., 2011; Wu et al., 2015]. This may result from heterogeneity and limited number of the available *Landsat* scenes or from the greater initial dust content caused by low summer precipitation in the 1990s (below the average level). No cumulative effect of dust on the ice surface is traceable either over the Ak-Shyirak area [Torgoev, 2017]. This inference is consistent with independent estimates of 3–4 ton daily mining-related dust emission in the Kumtor [Torgoev and Aleshin, 2001; Torgoev, 2017], or about 1000 tons annually, and 1 m/1000 years (1000 m³/km²) aeolian dust transport to the snow and ice areas of the Tien Shan [Stepanov, 1961]. Yet, dust emission by the Kumtor mining may cause just local effects on the albedo patterns.

CONCLUSIONS

Albedo of the glacier surface in the Ak-Shyirak massif has been estimated using ground-based and remote sensing data. Field surveys were performed in five glaciers in the summer of 2015 and in two glaciers located close to the area. In all cases, the albedo values varied within 0.16–0.18. Correlating the ground-based values to satellite data was impossible due to weather instability. In the summer of 2016, additional surveys were performed at six glaciers in Kyrgyzstan, and the satellite passed over the area on the dates of ground measurements in two cases. The available algorithms for *Landsat* data processing were analyzed after converting the acquired data to the earth's surface reflectance. The *Landsat* data were chosen for their high resolution (30 m/pixel), according to recommendations for estimating the radiation properties of mountain glaciers [Pope and Rees, 2014]. The albedo values fitted the best the observations when calculated with the equation from [Duguay and LeDrew, 1992]: the correlation coefficient $R = 0.81$ and the standard deviation $\sigma = 0.02$.

We have suggested a model using albedo estimates from satellite data corrected with reference to ground-based measurements. Only 27 *Landsat* scenes were suitable for the study according to weather conditions, out of more than 200 images covering the whole Ak-Shyirak area. At the final step, calculations over the selected scenes yielded albedo over the Ak-Shyirak glaciers, at >400,000 points each corresponding to one pixel, or a 30 × 30 m² of the surface.

Unlike glaciers in some other high mountain regions, the albedo values obtained for the Ak-Shyirak massif have not shown decreasing trends since the 1990s. The albedo patterns in the area have mostly driven by environmental factors like seasonality, elevation and weather conditions in the preceding season. The *Landsat*-derived albedo of the Ak-Shyirak glaciers does not correlate with distance to the central pit at the Kumtor gold field. No mining-induced

dust pollution of glaciers is detectable against the natural background, though some local albedo minima within the pit and in its vicinity may be caused by displacement of ice and its mixing with and burial under waste rock, as well as by dusting at the site.

We greatly appreciate logistic support by the management of Kumtor Gold Company. We wish to thank personally E.T. Kozhomkulov, S.S. Kutuzov (Institute of Geography, Moscow), V.V. Popovnin (Moscow State University), V.I. Shatravin, and R. Satylkanov (Institute of Water Problems and Water Power Industry, Kyrgyz Republic, Bishkek) for discussions. Field albedo measurements were organized with the aid of S.A. Erokhin (Institute of Water Problems and Water Power Industry, Bishkek) on the Adygene glacier, as well as M. Barandun, T. Saks, and H. Mahgut (Freiburg University, Switzerland) on the West Suyok, No. 354, Abramov, and Golubin glaciers. The manuscript profited from constructive critics by anonymous reviewers.

The methods for using Landsat scenes for estimating albedo were developed under support from the Russian Foundation for Basic Research (Project 18-05-00838). The study was carried out as part of government assignments 1.5. "Cryosphere Change under Environmental and Technogenic Impacts" and 1.20 "Mapping, Geoinformatics, and Remote Sensing for Global Climate and Social Change: Methods and Technologies".

References

- Aoki, T., Motoyoshi, H., Kodama, Y., et al., 2007. Variations of snow physical parameters and their effects on albedo in Sapporo, Japan. *Ann. Glaciol.* 46, 375–281.
- As, D.V., Hubbard, A., Hasholt, B., et al., 2012. Large surface meltwater discharge from the Kangerlussuaq sector of the Greenland ice sheet during the record warm year 2010 explained by detailed energy balance observations. *The Cryosphere*, No. 6, 199–209.
- Brest, C.L., Goward, S.N., 1987. Deriving surface albedo measurements from narrow band satellite data. *Intern. J. Remote Sensing*, No. 8 (3), 351–367.
- Brock, B.W., Willis, I.C., Sharp, M.J., 2000. Measurement and parameterization of albedo variations at Haut Glacier d'Arolla. Switzerland *J. Glaciol.* 46 (155), 675–688.
- Dozier, J., Green, R., Nolin, A., Painter, T., 2009. Interpretation of snow properties from imaging spectrometry. *Remote Sensing of Environ.* 113, S25–S37.
- Duguay, C.R., LeDrew, E.F., 1992. Estimating surface reflectance and albedo over rugged terrain from Landsat-5 Thematic Mapper over Rugged Terrain. *Photogrammetric Eng. and Remote Sensing* 58 (5), 551–558.
- Dumont, M., Durand, Y., Arnaud, Y., Six, D., 2011. Variational assimilation of albedo in a snowpack model and reconstruction of the spatial distribution of an alpine glacier. *J. Glaciol.* 58 (207), 151–164.
- Franch, B., Vermote, E.F., Claverie, M., 2014. Intercomparison of Landsat albedo retrieval techniques and evaluation against in situ measurements across the US SURFRAD network. *Remote Sensing of Environ.* 152, 627–637.

- Fujita, K., 2008a. Influence of precipitation seasonality on glacier mass balance and its sensitivity to climate change. *Ann. Glaciol.* 48, 88–92.
- Fujita, K., 2008b. Effect of precipitation seasonality on climatic sensitivity of glacier mass balance. *Earth and Planet. Sci. Lett.* 276 (1–2), 14–19.
- Fujita, K., Ageta, Y., 2000. Effect of summer accumulation on glacier mass balance on the Tibetan Plateau revealed by mass balance model. *J. Glaciol.* 46 (153), 244–252.
- Glazovskaya, M.A., 1952. Fine-grained Aeolian Deposits on the Terskey Alatau Glaciers. *Transactions, Moscow, Institute of Geography*, 49 pp. (in Russian)
- Jin, Z., Charlock, T.P., Yang, P., Xie, Y., Miller, W., 2008. Snow optical properties for different particles shapes with application to snow grain size retrieval and MODIS/CERES radiance comparison over Antarctica. *Remote Sensing of Environ.* 112, 3563–3581.
- Kaulbars, A.V., 1875. Data on the Tien Shan geography collected during a trip. In: *Reports of the Russian Geographical Society, General Geography*, vol. 5, 253–539. (in Russian)
- Knap, W.H., Brock, B.W., Oerlemans, J., Willis, I.C., 1999. Comparison of Landsat TM-derived and ground-based albedo of Haut Glacier d'Arolla, Switzerland. *Intern. J. Remote Sensing*, 20, 3293–3310.
- Konovalov, V.G., 1985. Snow Melting and Glacier Runoff. *Gidrometeoizdat, Leningrad*, 121 pp. (in Russian)
- Kronenberg, J., 2013. Linking ecological economics and political ecology to study mining, glaciers and global warming. *Environ. Policy and Governance* 23, 75–90.
- Kuzmichonok, V.A., 2012. Dust content in the atmosphere and glaciers in the area of the Kumtor Deposit (Ak-Shyirak, Tien Shan). *Led i Sneg (Ice and Snow)*, No. 2, 131–140.
- Li, Z.Q., Li, H.L., Chen, Y.N., 2011. Mechanisms and simulation of accelerated shrinkage of continental glaciers: a case study of Urumqi Glacier No. 1 in Eastern Tianshan, Central Asia. *J. Earth Science* 22 (4), 423–430.
- Liang, S., 2001. Narrowband to broadband conversions of land surface albedo and algorithms. *Remote Sensing of Environ.* 76, 213–238.
- Liang, S., Shuey, J.C., Russ, A.L., et al., 2003. Narrowband to broadband conversions of land surface albedo: II. Validation. *Remote Sensing of Environ.* 84, 25–41.
- Lucht, W., Hyman, A.H., Strahler, A.H., et al., 2000. A comparison of satellite-derived spectral albedo to ground-based broadband albedo measurements modeled to satellite spatial scale for a semidesert landscape. *Remote Sensing of Environ.* 74, 85–98.
- Naegeli, K., Damm, A., Huss, M., et al., 2017. Cross-comparison of albedo products for glacier surfaces derived from airborne and satellite (Sentinel-2 and Landsat 8) optical data. *Remote Sensing*, No. 9, 110–132.
- Oerlemans, J., Knap, W.A., 1998. 1 year record of global radiation and albedo in the ablation zone of Morteratschgletscher, Switzerland. *J. Glaciol.* 44, 231–238.
- Oerlemans, J., Giesen, R., Van Den Broeke, M., 2009. Retreating alpine glaciers: increased melt rates due to accumulation of dust (Vadret da Morteratsch, Switzerland). *J. Glaciol.* 55 (192), 729–736.
- Petrakov, D., Shpuntova, A., Aleinikov, A., et al., 2016. Accelerated glacier shrinkage in the Ak-Shyirak massif, inner Tien Shan, during 2003–2013. *Sci. Total Environ.* 562, 364–378.
- Pimentel, R., Aguilar, C., Herrero, J., et al., 2016. Comparison between snow albedo obtained from Landsat TM, ETM+ Imagery and the SPOT VEGETATION albedo product in a Mediterranean Mountainous site hydrology. *Hydrology* 3 (10), 1–19.
- Pope, A., Rees, W.G., 2014. Impact of spatial, spectral, and radiometric properties of multispectral imagers on glacier surface classification. *Remote Sensing of Environ.* 141, 1–13.
- Solar Radiation Measurements – Kipp&Zonen. – URL: <http://www.kippzonen.com> (submittal date: 22.03.2018).
- SP Lite 2 Pyranometer. Instruction Manual. June 2015. – URL: https://s.campbellsci.com/documents/ca/manuals/splite2_man.pdf (submittal date: 22.03.2018).
- Stepanov, I.N., 1961. Snow patches in the Tien Shan. *Priroda (Nature)*, No. 1, 109–110.
- Storey, J., Choate, M., Lee, K., 2014. Landsat 8 operational land imager on-orbit geometric calibration and performance. *Remote Sensing* 6, 11127–11152.
- The Eppley Laboratory. – URL: <http://www.eppleylab.com> (submittal date: 22.03.2018).
- Torgoev, I.A., 2017. *Glaciers, Gold and Geoenvironment of Kumtor*. LAP Lambert Academic Publishing, Riga, 204 pp. (in Russian)
- Torgoev, I.A., Aleshin, Yu.G., 2001. *Environmental Issues of Mining and Ore Processing in Kyrgyzstan*. Ilim, Bishkek, 239 pp. (in Russian)
- USGS Product Guide: Landsat 4-7 Climate Data Record (CDR) Surface Reflectance. Version 7.0. 2016. – URL: https://landsat.usgs.gov/sites/default/files/documents/ledaps_product_guide.pdf (submittal date: 22.03.2018).
- Warren, S.G., 1982. Optical properties of snow. *Rev. Geophysics* 20, 67–89.
- What are the band designations for the Landsat satellites? – URL: <https://landsat.usgs.gov/what-are-band-designations-landsat-satellites> (submittal date: 22.03.2018).
- Wu, X., Wang, N., Lu, An., et al., 2015. Variations in albedo on Dongkemadi Glacier in Tanggula Range on the Tibetan Plateau during 2002–2012 and its linkage with mass balance. *Arctic, Antarctic, and Alpine Res.* 47 (2), 71–82.

Received March 26, 2018

Revised version received December 10, 2018

Accepted December 19, 2018